

A massively parallel evolutionary algorithm for the partial Latin square extension problem

Olivier Goudet and Jin-Kao Hao*

LERIA, University of Angers, 2 Boulevard Lavoisier, 49045 Angers, France

Abstract

The partial Latin square extension problem is to fill as many as possible empty cells of a partially filled Latin square. This problem is a useful model for a wide range of applications in diverse domains. This paper presents the first massively parallel evolutionary algorithm for this computationally challenging problem based on a transformation of the problem to partial graph coloring. The algorithm features the following original elements. Based on a very large population (with more than 10^4 individuals) and modern graphical processing units, the algorithm performs many local searches in parallel to ensure an intensive exploitation of the search space. The algorithm employs a dedicated crossover with a specific parent matching strategy to create a large number of diversified and information-preserving offspring at each generation. Extensive experiments on 1800 benchmark instances show a high competitiveness of the algorithm compared to the current best performing methods. Competitive results are also reported on the related Latin square completion problem. Analyses are performed to shed lights on the roles of the main algorithmic components. The code of the algorithm will be made publicly available. *Keywords:* Combinatorial optimization, evolutionary search, parallel search, heuristics, partial graph coloring, Latin square problems.

1 Introduction

A Latin square \mathcal{L} of order n , also called a Quasigroup, is an $n \times n$ grid filled with n distinct symbols $\{1, \dots, n\}$, where each symbol appears exactly once in each row and column of the grid (Latin square condition). A partial Latin square of order n verifies that each cell is either empty or contains one of the n symbols, and each symbol occurs at most once in any row or column. Given

* Corresponding author.

Email addresses: olivier.goudet@univ-angers.fr (Olivier Goudet),
jin-kao.hao@univ-angers.fr (Jin-Kao Hao).

a partial Latin square, the partial Latin square extension (PLSE) problem is to fill as many as possible the empty cells. The Latin square completion (LSC) problem (also called Quasigroup completion problem) is the decision version that determines whether it is possible to fill all the empty cells of a partial Latin square. Figure 1 shows a PLSE instance with $n = 3$. Numbers in red correspond to filled cells. Two different optimal solutions with a score of 7 are displayed (it is impossible to complete the grid).

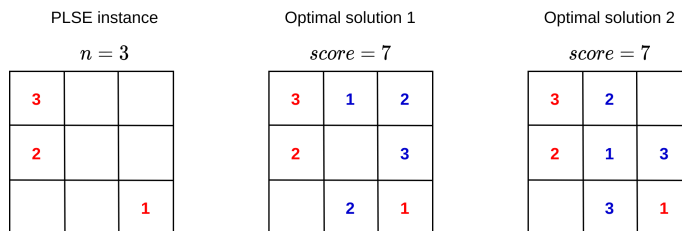


Fig. 1. Example of a PLSE instance with $n = 3$.

Latin square problems naturally appear in numerous applications, such as scheduling, error correcting codes, as well as experimental and combinatorial design [1,2]. For instance, a typical application of the PLSE is the design of optical router systems [3]. Optical routers are connected by optical links supporting a number of wavelengths. Each router has n input and n output links, and is capable of switching wavelengths to avoid conflicts in optical links. As displayed on Figure 2, the connections between input and output links can be modeled by a $n \times n$ array, where the n rows and n columns correspond to the inputs and the n outputs respectively. Each element at the position (i, j) can be filled by a number in $\{1, \dots, n\}$ indicating a specific wavelength used for the connection between input port i and output port j . In order to avoid wavelength conflicts, it is mandatory that each input or output port does not use the same frequency for more than one communication. Empty connections between input and output are indicated with empty cells. Given a router with existing connections between inputs and outputs, adding as many as new connections without introducing conflicts in the router is to solve the associated partial Latin square extension problem.

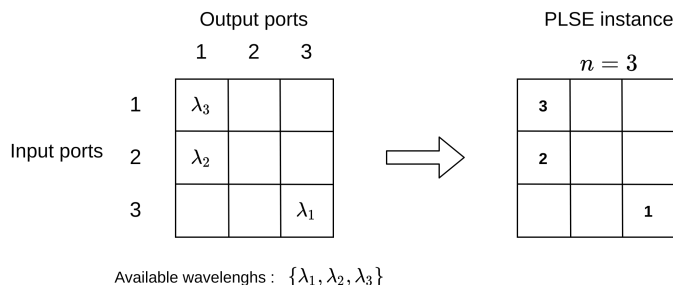


Fig. 2. Example of the optical router extension problem with $n = 3$ converted to the partial Latin square extension problem.

The LSC is known to be NP-complete [4]. As the result, both the decision

problem (LCS) and the optimization problem (PLSE) are computationally challenging in the general case. Due to their importance, Latin square problems have been studied from a wide variety of perspectives in different fields.

In algebra, the multiplication table of a finite quasigroup corresponds to a Latin square [5]. As such, Latin squares have been studied as a mathematical object and various properties were established [6,7,8].

The LSC can be expressed as an integer program with n^3 Boolean variables $x_{i,j,k}$, where $x_{i,j,k} = 1$ indicates that the cell in position (i, j) receives the symbol $k \in \{1, \dots, n\}$. With this formulation and using integer programming solvers, optimal results were reported for small instances in [9]. The authors also investigated two other exact methods based on constraint programming (CP) and SAT technologies. A systematic comparison of SAT and CP models was presented in [10]. An approximation algorithm was proposed based on a packing integer programming formulation in [11].

In terms of practically solving the PLSE, a notable work was presented in [12]. In this work, a partial Latin square was represented by means of an orthogonal array, with a set of triples in $[n]^3$, such that each element (v_1, v_2, v_3) of this set indicates that the symbol v_3 is assigned to (v_1, v_2) . The Hamming distance between each pair of elements of this set is then computed. If the distance between each pair of triples of this set is at least two, this set corresponds to a partial Latin square. Based on this representation, the author proposed several iterated local search algorithms which aim to extend the current set of triples without adding conflicts. To assess the practical performance of these iterated local search algorithms, the author introduced a set of 1800 instances for the PLSE and another set of 1800 instances for the LSC with various characteristics (cf. Section 4.1 and Appendix B). Computational results showed that the iterated local search algorithms perform extremely well by outperforming previous methods including integer programming, constraint programming as well as their hybridized approach.

The problem of extending a partial Latin square can also be studied under the view of (partial) graph coloring [13]. Indeed, a partial Latin square of order n can be transformed to a graph such that each vertex (or node) corresponds to a cell of the grid (there are thus n^2 vertices), and an edge exists between two vertices corresponding to two cells of the same row or column (there are thus $n^2(n - 1)$ edges). The vertex of a pre-filled cell with a symbol k receives color $k \in \{1, \dots, n\}$. Empty cells are left uncolored. The PLSE is to color as many uncolored vertices as possible such that two colored vertices do not share the same color. Based on this observation, the authors of [14] proposed a powerful memetic algorithm (MMCOL) for the Latin square completion problem and solved all the 1800 LSC instances introduced in [12] as well as all the 19 traditional LSC instances in the literature [9]. With some slight adaptations

of their algorithm, they also reported excellent results on the 1800 PLSE instances of [12].

To sum, the two most recent studies on the PLSE [12] and the LSC [14] significantly contributed to the practical solving of these two challenging problems. In particular, all the existing LSC benchmark instances have been solved thanks to the algorithm presented in [14]. On the contrary, this is not the case for the PLSE and there is still room for improvement in terms of better solving the PLSE instances. In fact, for almost half of the 1800 benchmark instances, their optimal solutions are still unknown and only lower bounds were reported.

This work is motivated by this observation, and aims to advance the state-of-the-art of solving the PLSE by establishing record-breaking lower bounds for the unsolved PLSE instances. For this purpose, we introduce the first massively parallel evolutionary algorithm that fully takes advantage of the GPU architecture to parallelize all critical search components. We summarize the contributions of this work as follows.

From the perspective of algorithm design, the proposed algorithm relies on a very large population P ($|P| > 10^4$) that enables massively parallel local optimization and offspring generation on the GPU architecture. This is in sharp contrast to the typical use of a small population P (typically $|P| < 10^2$) and sequential computations of many memetic algorithms including the MMCOL algorithm [15,16,14]. The algorithm features several complementary and original search components including a parametrized asymmetric uniform crossover and an effective local search. The crossover uses a probability to control the inherited information from the parents according to a distance metric and a specific parent matching strategy to create a large number of diversified and information-preserving offspring. The local search utilizes a two-phase approach to effectively explore an enlarged search space. The algorithm is further reinforced by a parallel distance calculation procedure that enables a fast population updating.

From the perspective of computational performance, we demonstrate a high competitiveness of our algorithm on the 1800 PLSE benchmark instances from [12]. We report many improved best lower bounds for large and difficult instances, including 25 record optimal solutions. We also test the algorithm on the related LSC and show that the algorithm is able to solve all the existing benchmark instances (1800 from [12] and 19 from [9]).

Finally, we contribute to the understanding of the population size, the crossover and the parent matching strategy for a large population. In particular, we show that the random parent matching strategy which is typically employed in many memetic algorithms (e.g., [17,14]) is no more suitable in the context of a large population and can be beneficially replaced by a neighborhood

matching strategy for a better efficiency.

In the rest of the paper, we present the solution approach and the proposed algorithm (Sections 2 and 3), experimental results and comparisons with the state-of-the-art methods (Sections 4), followed by analyses of key algorithmic components and conclusions (Sections 5 and 6).

2 Partial Latin square extension as graph coloring

This section illustrates how the partial Latin square extension problem can be considered as a graph coloring problem. This approach was first used in [14] with a great success to solve the related Latin square completion problem. However, two specific and significant features of the partial Latin square extension problem were ignored until now. We discuss them at the end of this section, which also provide additional motivations for this work.

2.1 Partial Latin square extension to Latin square graph

Let \mathcal{L} be a Latin square of order n composed of $n \times n$ cells. \mathcal{L} can be transformed into a graph $G = (V, E)$, called Latin square graph, with the vertex set $V = \{\{1, \dots, n\} \times \{1, \dots, n\}\}$ of size $|V| = n^2$ and the edge set E of size $|E| = n^2(n - 1)$ where $\{u, v\} \in E$ if and only if u and v are two vertices representing two cells of the same row or same column of \mathcal{L} [13,14]. Then solving the PLSE can be reached by finding a partial legal n -coloring (also called list-coloring [13]) of the graph G by using the colors in $\{1, \dots, n\}$ while maximizing the number of colored vertices (or equivalently minimizing the number of uncolored vertices).

Let $D(v)$ denote the color domain of vertex v (i.e., the set of colors that can be used to color v). If v corresponds to a cell pre-filled with symbol k ($k \in \{1, \dots, n\}$), $D(v) = \{k\}$. If v corresponds to an empty cell, v can receive a color in $\{1, \dots, n\}$ or remain uncolored, indicated with the color 0. In other words, $D(v) = \{0, 1, \dots, n\}$ for any vertex v representing an empty cell. Then a (partial) legal n -coloring of the associated Latin square graph G is a function $S : V \rightarrow \{D(v_1), \dots, D(v_{|V|})\}$ such that for any pair of vertices u and v , if $S(u) \neq 0$, $S(v) \neq 0$, and they are linked by an edge ($\{u, v\} \in E$), then their colors $S(u)$ and $S(v)$ must be different ($S(u) \neq S(v)$). Note that a vertex receiving color 0 indicates an uncolored vertex.

A legal solution of the PLSE can also be seen as a partition of V into n disjoint stable sets V_1, V_2, \dots, V_n and a set $V_0 = V \setminus \cup_{i=1}^n V_i$, such that V_i is

the set of vertices receiving color i . A set V_i ($i = 1, \dots, n$) is a stable set if $\forall (u, v) \in E, \{u, v\} \notin E$. A stable set is also called a color class.

Let $S = \{V_0, V_1, V_2, \dots, V_n\}$ be a partition of the vertex set V , the objective of the partial Latin square extension problem (PLSE) in terms of the list-coloring problem can be stated as follows:

$$\text{minimize } f(S) = |V_0| \tag{1}$$

$$\text{subject to } \forall u, v \in V_i, \{u, v\} \notin E, i = 1, 2, \dots, n \tag{2}$$

where the objective (1) is to minimize the cardinality of the set V_0 (number of uncolored vertices) and the constraints (2) ensure that the partition $\{V_0, V_1, V_2, \dots, V_n\}$ is a legal but potentially partial n -coloring. Notice that this formulation of the partial Latin square extension problem can also be used to solve the Latin square completion problem (LSC), for which a legal solution S with $f(S) = 0$ is sought.

The constraints (2) can be reformulated with a constraint function c which simply counts the number of conflicts in S :

$$c(S) = \sum_{\{u,v\} \in E} \delta_{uv}, \tag{3}$$

where

$$\delta_{uv} = \begin{cases} 1 & \text{if } u \in V_i, v \in V_j, i = j \text{ and } i \neq 0 \\ 0 & \text{otherwise.} \end{cases} \tag{4}$$

If $\delta_{uv} = 1$, u and v are two conflicting vertices (i.e., they receive the same colors while they are adjacent in the graph). Clearly, a coloring S with $c(S) = 0$ corresponds to a legal n -coloring.

Figure 3 shows a PLSE instance (left), its Latin square graph (middle) and a legal partial coloring of the Latin square graph with two uncolored vertices (color 0) (right).

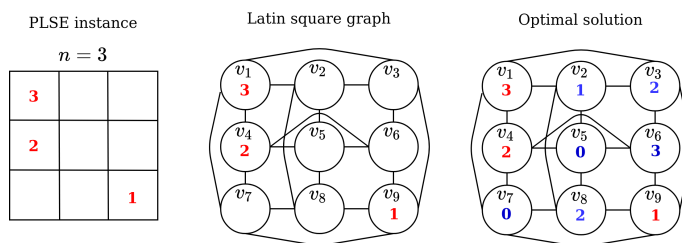


Fig. 3. Example of converting a partial Latin square extension instance (left) to a Latin square graph (middle) and an optimal partial coloring with two uncolored vertices (color 0) (right).

2.2 Preprocessing of the Latin square graph

As indicated in [14], a preprocessing procedure can be applied to reduce a Latin square graph by removing the colored vertices (i.e., the filled cells). Indeed, if a vertex v of the graph represents a cell pre-filled with symbol $k \in \{1, \dots, n\}$, the vertex definitively receives this unique color k and can be removed from the graph. Moreover, since the color k cannot be assigned to any vertex u adjacent to v (i.e., $\{u, v\} \in E$), this color can thus be safely removed from the color domain $D(u)$ (in order to respect the Latin square condition).

Nevertheless, during the preprocessing, if the color domain of a vertex u becomes the singleton $D(u) = \{0\}$, it means that the corresponding cell cannot be filled. This cell remains definitively unfilled and the vertex u is removed from the graph. If one denotes by l the number of cells impossible to fill after this preprocessing phase, $n^2 - l$ defines an upper bound of the optimal value (score) of the given PLSE instance. For the special case of $l = 1$, a better upper bound is in fact $n^2 - 2$, as there is no optimal solution for a PLSE instance with a score of $n^2 - 1$ (cf. Theorem 6 in [18]).

Algorithm 1 Preprocessing procedure for graph reduction of the PLSE problem

```

1:
2: Input: A Latin square graph  $G = (V, E)$  with some vertices already colored,
   each vertex  $v$ 's color domain  $D(v)$ .
3: Output: A reduced graph and the number  $l$  of cells impossible to fill.
4:
5: for each vertex  $v \in V$  with singleton color domain  $D(v) = \{k\}$  do
6:    $V \leftarrow V - \{v\}$  // Remove this colored vertex  $v$  from the graph
7:    $E \leftarrow E - \{\{u, v\} \in E\}$  // Remove the edges linked to  $v$ .
8:   for each uncolored  $u \in V$  adjacent to  $v$  do
9:      $D(u) \leftarrow D(u) - \{k\}$  // Remove color  $k$  from the color domain  $D(u)$ 
10:  end for
11: end for
12:
13:  $l = 0$ 
14: for each  $v \in V$  do
15:   if  $D(v) = \{0\}$  then
16:      $l = l + 1$ 
17:      $V \leftarrow V - \{v\}$  // Remove this node impossible to color
18:      $E \leftarrow E - \{\{u, v\} \in E\}$  // Remove the edges linked to  $v$ .
19:   end if
20: end for

```

Figure 4 (Right) displays the reduced graph of the Latin square graph shown in Figure 3. Numbers in accolades indicate the color domain $D(v_i)$ of each vertex v_i . In addition to the three precolored vertices v_1, v_4, v_9 , vertex v_7 is

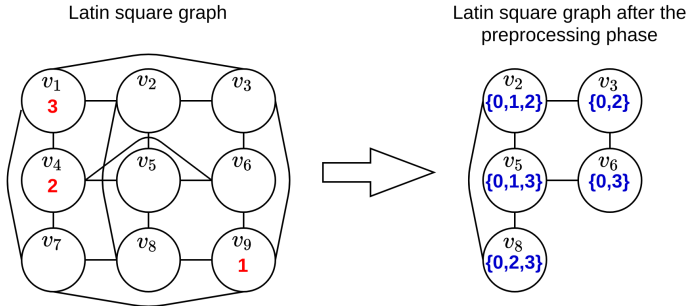


Fig. 4. Preprocessing of a Latin square graph with $n = 3$.

also removed because its color domain is $D(v_7) = \{0\}$. Therefore, $l = 1$, leading to an upper bound $3^2 - 2 = 7$. Since this upper bound is equal to the lower bound of the two solutions of Figure 1, these two solutions are proven to be optimal for the given PLSE instance (i.e., the maximum of 7 filled cells / colored vertices or the minimum of 2 unfilled cells / uncolored vertices).

2.3 Special features of the transformed coloring problem

One observes two special features of the graph coloring problem transformed from the PLSE.

First, the Latin square graph coloring problem is a list-coloring problem [13], where the permissible colors of a vertex are limited to a list of colors in $\{0, 1, \dots, n\}$, instead of the whole set $\{0, 1, \dots, n\}$. Therefore, contrary to the standard graph coloring problem, candidate solutions are in general not invariant by permutation of colors. For example, in the legal partial coloring shown on Figure 3 on the right, it is impossible to swapping colors 2 and 3 as the color 2 is not in the domain of the vertex v_6 . Moreover, even a permissible color exchange between two colorings is not generally neutral. For example, consider the two legal solutions S_1 and S_2 displayed on Figure 5, where the pre-filled colors are in red, assigned colors are in blue and possible color changes are in green. The solution S_2 is the same as the solution S_1 except that the colors 1 and 3 are swapped. After this swap, it becomes impossible to change the color of the vertex v_2 in S_2 while it was possible in S_1 . S_1 and S_2 are thus two different candidate solutions for the PLSE, while they represent the same coloring for the conventional graph coloring problem. This observation implies that for this list-coloring problem, solutions are not invariant by permutation of the colors. As a result, the so-called set-theoretic partition distance [19], which is usually used to measure the distance between two solutions for graph coloring [20,21], is not meaningful for the list-coloring problem. Instead, the Hamming distance D^H is more suitable to measure the distance between solutions for our coloring problem (cf. Section 3.4).

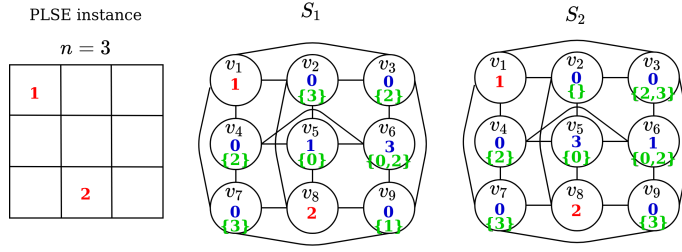


Fig. 5. Two legal solutions S_1 and S_2 of the PLSE instance. The two solutions are the same except that the colors 1 and 3 are swapped.

Secondly, the partial list-coloring from the PLSE aims to find a legal coloring such that the objective function $f(S)$ defined by equation (1) (number of uncolored vertices) is minimized. Therefore, it is critical that the algorithm is able to decide which vertices are to be left uncolored when it is impossible to color all the vertices of the graph.

For these reasons, we introduce an algorithm specifically designed to solve the list-coloring problem of Latin square graphs of the PLSE. This algorithm, presented in the next section, can also be applied to solve the related Latin square completion problem (LSC).

3 Massively parallel memetic algorithm

We describe in this section the massively parallel memetic algorithm (MPMA) for coloring Latin square graphs.

3.1 Search space and evaluation function

The enlarged search space Ω explored by the MPMA algorithm is composed of the legal, illegal and potentially partial candidate solutions.

Let $G = (V, E)$ be the reduced Latin square graph with $|V|$ vertices $\{v_1, \dots, v_{|V|}\}$, and color domains $D(v_i) \subseteq \{0, 1, \dots, n\}$ ($i = 1, \dots, |V|$) obtained after the pre-processing phase. Then the space Ω is given by:

$$\Omega = \{S : V \rightarrow \{D(v_1), \dots, D(v_{|V|})\}\} \quad (5)$$

The MPMA algorithm aims to find a legal, possibly partial solution S (with $c(S) = 0$) of the Latin square graph with the minimum number of uncolored vertices $f(S)$ (for functions f and c , see Section 2.1).

Following the general idea of penalty function for constrained optimization [22,23,24], we define the following extended evaluation function F (to be minimized) to assess the quality (fitness) of a candidate solution $S \in \Omega$:

$$F(S) = f(S) + \phi c(S) \quad (6)$$

where $\phi > 0$ is a penalty parameter controlling the impact of the constraint function c on the overall score. Generally, decreasing the value of ϕ favors solutions with less uncolored vertices and more conflicts, while increasing its value promotes legal (conflict-free) and partial colorings. If ϕ is set to the value of 1, x uncolored vertices and x conflicts contribute equally to the quality of the solution.

3.2 Main scheme

The proposed MPMA algorithm relies on the population-based memetic framework [25], which has been applied to several graph coloring problems [17,26,21,27]. It's worth noting that these memetic algorithms typically use a small population with no more than 20 individuals and are elitist evolutionary algorithms. As such, each generation usually creates one or two offspring solutions via a crossover operator, which are further improved by a local search procedure.

The massively parallel memetic algorithm proposed in this work uses a very large population P ($|P| \geq 10^4$), whose individuals evolve in parallel in the search space. This approach secures a desirable high degree of population diversity, which in turn favors a large exploration of the candidate solutions. In order to take advantage of this large population, we leverage the computing power of modern GPUs to perform parallel computations at each generation: local searches, distance evaluations and crossovers. The only part which remains sequential is the population update operation that merges the current population and the offspring population to create the next population.

The algorithm takes a reduced Latin square graph G (cf. Section 2.2) as input and tries to find a legal, possibly partial, coloring with a minimum number of uncolored vertices. The pseudo-code of MPMA is shown in Algorithm 2, while its flowchart is displayed in Figure 7. At the beginning, all the individuals of the population are initialized at random in parallel. Then, the algorithm repeats a loop (generation) until a stopping criterion (e.g., a cutoff time limit or a maximum of generations) is met. Each generation t involves the execution of four components:

- (1) The p individuals (illegal n -colorings) of the current population are simultaneously improved by running in parallel a two-phase local search (cf. Section 3.3) to minimize the fitness function f (uncolored vertices)

Algorithm 2 Massively parallel memetic algorithm for Latin square graph coloring

```

1: Input: Reduced Latin square graph  $G = (V, E)$ , population size  $p$ , color domain
    $D(v)$  of each vertex  $v \in V$ .
2: Output: The best legal partial coloring  $S^*$  found
3:  $P = \{S_1, \dots, S_p\} \leftarrow$  population_initialization
4:  $S^* = \emptyset$  and  $e(S^*) = |V|$ .
5:  $\{S_1^O, \dots, S_p^O\} \leftarrow \{S_1, \dots, S_p\}$ 
6: repeat
7:   for  $i = \{1, \dots, p\}$ , in parallel do
8:      $S'_i \leftarrow$  two-phase_local_search( $S_i^O$ )           /* Section 3.3
9:   end for
10:   $S'^* = \operatorname{argmin}\{f(S'_i), i = 1, \dots, p\}$ 
11:  if  $f(S'^*) < f(S^*)$  then
12:     $S^* \leftarrow S'^*$ 
13:  end if
14:   $D \leftarrow$  distance_computation( $S_1, \dots, S_p, S'_1, \dots, S'_p$ ) /* Section 3.4
15:   $\{S_1, \dots, S_p\} \leftarrow$  pop_update( $S_1, \dots, S_p, S'_1, \dots, S'_p, D$ ) /* Section 3.4
16:   $\{S_1^O, \dots, S_p^O\} \leftarrow$  build_offspring( $S_1, \dots, S_p, D$ ) /* Section 3.5
17: until stopping condition met
18: return  $S^*$ 

```

and the constraint function c (conflicting vertices).

- (2) The distances between all pairs of the existing individuals and the individuals improved by local search are computed in parallel (cf. Section 3.4).
- (3) Then the population updating procedure (cf. Section 3.4) merges the $2p$ existing and new individuals to update the population, by taking into account the fitness f of each individual (number of uncolored vertices) and the distances between individuals in order to maintain a healthy diversity of the population.
- (4) Finally each individual is matched with its nearest neighbor individual in the population and p crossovers are performed in parallel to generate p offspring solutions (cf. Section 3.5), which are improved by the parallel iterated local search during the next generation ($t + 1$).

The algorithm stops when a predefined time condition is reached or an optimal solution S^* is found. S^* is an optimal solution if 1) $c(S^*) = 0$, $f(S^*) = 0$, and $l \neq 1$ (i.e., all empty cells are filled), or 2) $c(S^*) = 0$, $f(S^*) = 1$, and $l = 1$ (the tightest upper bound is reached, see Section 2.2). If the algorithm does not find an optimal solution when it stops, it returns the best legal solution S^* (with $c(S^*) = 0$) found so far, with a number of unfilled cells $f(S^*) > 0$. Then the score $n^2 - l - f(S^*)$ is a lower bound of the given PLSE instance.

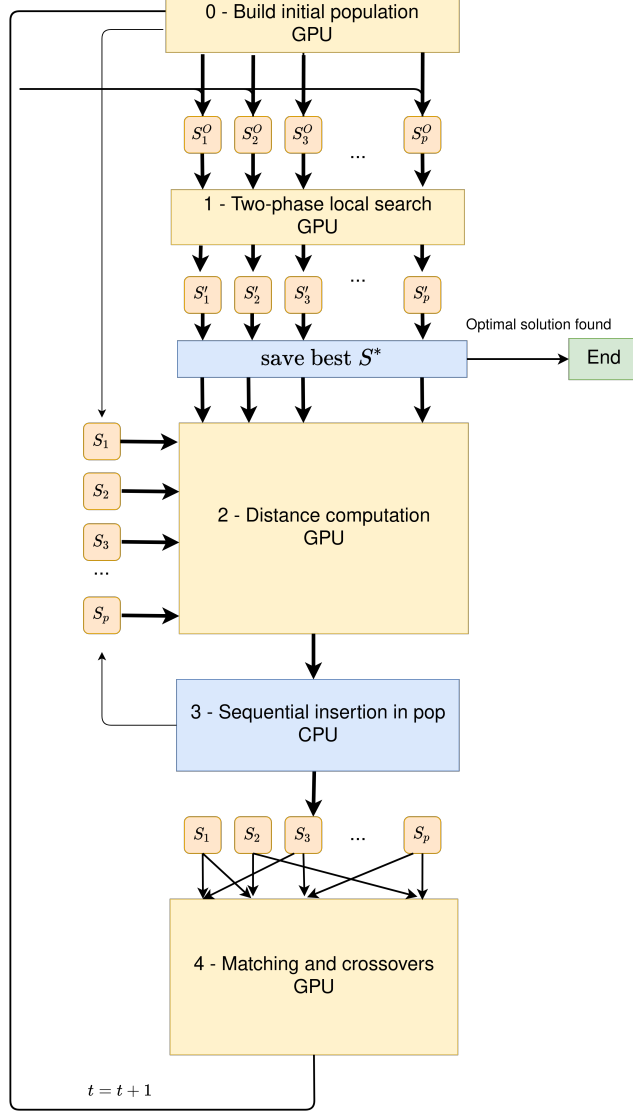


Fig. 6. General scheme of the MPMA algorithm.

3.3 Parallel two-phase local search

MPMA employs a two-phased partial legal and illegal tabu search (PLITS) to simultaneously improve in parallel the individuals of the current population. Specifically, PLITS relies on the tabu search metaheuristic to explore candidate solutions of the space Ω guided by the extended fitness function F given by equation (6). Indeed, tabu search is a popular method for graph coloring [28,24,29] and often used as the local optimization components of memetic algorithms [14,21,30].

Given a solution $S = \{V_0, V_1, V_2, \dots, V_n\}$, PLITS uses the one-move operator to displace a vertex v from its current color class V_i to a different color class V_j such that $i \neq j$ and $j \in D(v)$, leading to a neighboring solution denoted

as $S \oplus \langle v, V_i, V_j \rangle$. Let $\mathcal{C}(S)$ be the set of conflicting vertices in S , i.e., $\mathcal{C}(S) = \{v \in V_i : 1 \leq i \leq n, \exists u \in V_i, (u, v) \in E, u \neq v\}$. To make the examination of candidate solutions more focused, PLITS only considers the uncolored vertices in V_0 and conflicting vertices in $\mathcal{C}(S)$ for color changes.

The one-move neighborhood applied to the uncolored vertices of S is given by:

$$N_0(S) = \{S \oplus \langle v, V_0, V_j \rangle : v \in V_0, 1 \leq j \leq n, j \in D(v)\}$$

The one-move neighborhood applied to the conflicting vertices of S is given by:

$$N_c(S) = \{S \oplus \langle v, V_i, V_j \rangle : v \in \mathcal{C}(S), v \in V_i, 1 \leq i \leq n, \\ 0 \leq j \leq n, j \in D(v), i \neq j\}$$

Notice that a conflicting (colored) vertex can be moved to the set V_0 by the one-move operator, becoming thus uncolored.

PLITS explores the global one-move neighborhood:

$$N(S) = N_0(S) \cup N_c(S) \tag{7}$$

Specifically, PLITS makes transitions between various partial n -colorings with the help of the neighborhood $N(S)$ and the extended evaluation function F . It iteratively replaces the current solution S by a neighboring solution S' taken from $N(S)$, until a stopping condition is met. At each iteration, a best admissible neighboring solution S' is selected to replace S . After each iteration, the corresponding one-move is recorded in the tabu list to prevent the search from returning to a previously visited solution for the next T iterations (tabu tenure). Like [30], the tabu tenure depends on the number of vertices eligible for the one-move operator (i.e., $|V_0| + |\mathcal{C}(S)|$ in our case) and is set to the value of $L + \alpha(|V_0| + |\mathcal{C}(S)|)$, where L is a random integer from $[0; 9]$ and α is a parameter set to 0.6.

A neighboring solution S' is considered to be admissible if it is not forbidden by the tabu list or if it is better (according to the extended evaluation function F) than the best solution found so far. The neighborhood evaluations are performed incrementally using the streamline technique of [30]. As shown in Algorithm 3, we run in parallel the PLITS procedure on the GPU to raise the quality of the current population.

The PLITS procedure is performed in two phases with different search focuses. The first phase favors a large exploration of candidate solutions by setting ϕ to the value of 0.5 and performs $nbIter_{TS} = 100 * |V|$ iterations. The second phase focuses on resolving the conflicts in the solutions of the population to obtain P legal colorings (with $c(S) = 0$). For this purpose, ϕ is set to a large value of $|V|$ during $nbIter_{TS} = 2 * |V|$ iterations.

Algorithm 3 Parallel partial legal and illegal tabu search

```
1: Input: Population  $P = \{S_1, \dots, S_p\}$ , depth of tabu search  $nbIter_{TS}$ , color
   domain  $D(v)$  of each vertex  $v \in V$ .
2: Output: Improved population  $P' = \{S'_1, \dots, S'_p\}$ .
3: for  $i = \{1, \dots, p\}$ , in parallel do
4:    $S'_i \leftarrow S_i$  /* Records the best solution found so far on each local thread.
5: end for
6:  $iter = 0$ 
7: for  $i = \{1, \dots, p\}$ , in parallel do
8:   for  $t = \{1, \dots, nbIter_{TS}\}$  do
9:     Choose a neighboring solution  $S'_i \in N(S_i)$  which is not forbidden by the
       tabu list or better than  $S_i$  (according to the extended evaluation function
        $F$ ).
10:     $S_i \leftarrow S'_i$ 
11:    if  $F(S'_i) < F(S'_i)$  then
12:       $S'_i \leftarrow S'_i$ 
13:    end if
14:  end for
15: end for
16: return  $P' = \{S'_1, \dots, S'_p\}$ 
```

After the local search, the best coloring S'_i among the p conflict-free colorings in terms of the objective function f is used to update the recorded best solution S^* if $S'_i < S^*$.

3.4 Population update

The p new legal colorings from the PLITS procedure are used to update the population. For this, MPMA maintains a $p \times p$ matrix to record all the distances between any two solutions of the population. This symmetric matrix is initialized with the $p \times (p - 1)/2$ pairwise distances computed for each pair of individuals in the initial population, and then updated each time a new individual is inserted in the population.

To merge the p new solutions and the p existing solutions, MPMA needs to evaluate (i) $p \times p$ distances between each individual in the population $P = \{S_1, \dots, S_p\}$ and each improved offspring individual in $P' = \{S'_1, \dots, S'_p\}$ and (ii) $p \times (p - 1)/2$ distances between all the pairs of individuals in P' . All the $p \times p + p \times (p - 1)/2$ distance computations are independent from one another, and are performed in parallel on the GPU (one computation per thread).

Given two colorings S_i and S_j , MPMA uses the Hamming distance $D(S_i, S_j)$ to measure the dissimilarity between S_i and S_j , which corresponds to the

Algorithm 4 Sequential population update procedure

- 1: **Input:** Population $P_t = \{S_1, \dots, S_p\}$ (generation t) and offspring population $P' = \{S'_1, \dots, S'_p\}$ (generation t)
- 2: **Output:** Updated population P_{t+1} (generation $t + 1$)
- 3: $P_{t+1} = \emptyset$ /* Initialize new population
- 4: $P^{all} = P_t \cup P'$ /* Merge existing and improved new solutions
- 5: $S^{best} = \operatorname{argmin}_{S \in P^{all}} e(S)$ /* Identify the best legal solution in P^{all}
- 6: $P_{t+1} = P_{t+1} \cup \{S^{best}\}$ /* Add S^{best} in P_{t+1}
- 7: $P^{all} = P^{all} \setminus \{S^{best}\}$ /* Remove S^{best} from P^{all}
- 8: /* Add n -colorings in P_{t+1} until it contains the p best solutions of P^{all} with the condition that $D(S_i, S_j) > |V|/10$, for all $S_i, S_j \in P_{t+1}$, $i \neq j$
- 9: **while** $|P_{t+1}| < p$ **do**
- 10: $S^{best} = \operatorname{argmin}_{S \in P^{all}} e(S)$
- 11: $dist = \min_{A \in P_{t+1}} D(S^{best}, A)$
- 12: **if** $dist > |V|/10$ **then**
- 13: $P_{t+1} = P_{t+1} \cup \{S^{best}\}$
- 14: $P^{all} = P^{all} \setminus \{S^{best}\}$
- 15: **end if**
- 16: **end while**
- 17: **return** P_{t+1}

number of vertices that are colored differently in S_i and S_j :

$$D(S_i, S_j) = |\{v \in V, S_i(v) \neq S_j(v)\}| \quad (8)$$

Following [20], MPMA's population update procedure aims to keep the best individuals, but also to ensure a minimum spacing between the individuals. The population update procedure (Algorithm 4) greedily adds one by one the best individuals of $P^{all} = \{S_1, \dots, S_p\} \cup \{S'_1, \dots, S'_p\}$ in the population of the next generation P_{t+1} until P_{t+1} reaches p individuals, such that $D(S_i, S_j) > |V|/\gamma$ ($\gamma > 1.0$ is a parameter), for any $S_i, S_j \in P_{t+1}$, $i \neq j$.

3.5 Parent matching and crossover

At each generation, the MPMA algorithm performs in parallel p crossovers to generate p offspring solutions. For this, MPMA uses each existing solution in the current population as the first parent and selects another existing solution as the second parent with a specific parent matching strategy. The idea is to ensure that each individual in the population has a chance to transmit some *genetic information* to the next generation while encouraging the creation of diversified offspring.

3.5.1 Parent matching strategy

The population update strategy presented in the last section ensures that the individuals of the next population are of high quality, but also sufficiently distanced. This property provides a first basis to guarantee that for each of the p crossovers, we can find a second parent that is sufficiently distanced from the first parent. This contributes to building diversified offspring solutions that are different from their parents and thus helps the algorithm to continually explore new areas in the search space.

However, as we use a very large population, individuals can be highly different and share very little information. Indeed, we experimentally observed that the average pairwise distance in the population is usually very large, around $0.7 \times |V|$ even after many generations. Meanwhile, a study in [21] showed that for the standard graph coloring problem, crossing-over two highly different parents results in offspring of poor quality because no meaningful shared information can be transmitted from parents to offspring.

Thus, for each individual S_i (i.e., the first parent), we choose, among the other individuals in the population, the nearest neighbor S_j in the sense of the precomputed Hamming distance D , as the second parent.

3.5.2 Parameterized asymmetric uniform crossover

The popular greedy partition crossover (GPX) [30] and its variants have proven to be very successful for several graph coloring problems including the conventional graph coloring [17,21,31] and sum coloring [26]. GPX was also adapted to the related LSC, leading to maximum approximate group based crossover (MAGX) [14]. However, the GPX crossover has some limitations for the PLSE due to the fact that solutions are not invariant by permutations of color groups (cf. Section 2.3) and high-quality solutions do not share significant backbones (they are far away from each other, see Section 5).

For the PLSE, we introduce a parameterized asymmetric uniform crossover (AUX), which is easy to compute for a very large population of individuals and allows the transmission of favorable parental features to the next generation.

Given a first parent S_i and a second parent S_j , an offspring solution S_i^O is built such that each vertex v receives the color of S_i with probability p_{ij} and the color of S_j with probability $1 - p_{ij}$. The probability p_{ij} depends proportionally on the Hamming distance between the parents S_i and S_j and is given by:

$$p_{ij} = 1 - \frac{|V|}{\beta \times D(S_i, S_j)} \quad (9)$$

Algorithm 5 Parallel asymmetric uniform crossover AUX

- 1: **Input:** Population $P = \{S_1, \dots, S_p\}$, with $S_i = (V_0^i, V_1^i, \dots, V_n^i)$, for $i = 1, \dots, p$.
 - 2: **Output:** Offspring population $P^O = \{S_1^O, \dots, S_p^O\}$
 - 3: **for** $i = 1, \dots, p$, in parallel **do**
 - 4: $S_j \leftarrow$ Find and make a copy of the nearest neighbor of S_i from P according to the distance D such that $i \neq j$ and such that this crossover (i, j) has not been tested yet.
 - 5: $p_{ij} = 1 - \frac{|V|}{\beta \times D(S_i, S_j)}$
 - 6: **for** $l = \{1, \dots, |V|\}$ **do**
 - 7: With probability p_{ij} , $S_i^O(v_l) = S_i(v_l)$
 - 8: Otherwise $S_i^O(v_l) = S_j(v_l)$
 - 9: **end for**
 - 10: **end for**
 - 11: **return** P^O
-

where $\beta > 1.0$ is a real parameter controlling the degree of diversity of the resulting offspring.

As $|V|/\gamma$ is the minimum spacing between two individuals in the population (cf. Section 3.4), we set β such that $\beta > \gamma > 0$, in order to have $\forall i, j \in \llbracket 1, \dots, p \rrbracket^2, i \neq j, |V|/\beta < D(S_i, S_j)$. This ensures that $\forall i, j \in \llbracket 1, \dots, p \rrbracket^2, 0 < p_{ij} < 1$.

Notice that when p_{ij} is fixed to the value of 0.5, we obtain the classical Uniform Crossover (UX) [32]. With the UX crossover, the resulting offspring is on average equidistant from both parents. However, as we empirically show in Section 4, the UX crossover does not work well for the PLSE (it is too much disruptive). The proposed AUX crossover uses the probability p_{ij} to make itself more conservative by considering the distance between two parents. Specifically, if two parents are similar (with a small distance), the offspring can equally inherit information from the parents. On the contrary, if the parents are very different (with a large distance), it is preferable to conserve more information from one parent (the first parent) to avoid an offspring solution that is far away from both parents. AUX achieves this goal by adjusting the coefficient β which influences the probability.

For two given parents S_i and S_j , the expected distance between the offspring S_i^O and its first parent S_i is $\bar{D}(S_i, S_i^O) = |V|/\beta$. The expected distance between the offspring S_i^O and its second parent S_j is $\bar{D}(S_j, S_i^O) = D(S_i, S_j) - |V|/\beta$. If we choose $\beta \geq 2\gamma$, $\bar{D}(S_i, S_i^O) \geq \bar{D}(S_j, S_i^O)$ always holds. As such, in average the child preserves more genetic information from the first parent compared to the second parent. Given that MPMA uses every individual in the current population as the first parent, all individuals are offered the same chance to transmit a large part of their genetic information to their offspring, leading to a large coverage of the search space.

Figure 7 illustrates the creation of six offspring solutions $\{S_i^O\}_{i=1}^6$ (in red) generated from the population $\{S_i\}_{i=1}^6$ (in black). In this case, the offspring S_1^O to S_6^O are respectively generated from the ordered pairs of parents (S_1, S_2) , (S_2, S_3) , (S_3, S_4) , (S_4, S_5) , (S_5, S_4) , (S_6, S_1) .

As one notices, each offspring is situated in between its two parents in the search space and always closer to its first parent (in terms of the Hamming distance). The norm of each translation vector is equal to $|V|/\beta$ in average.

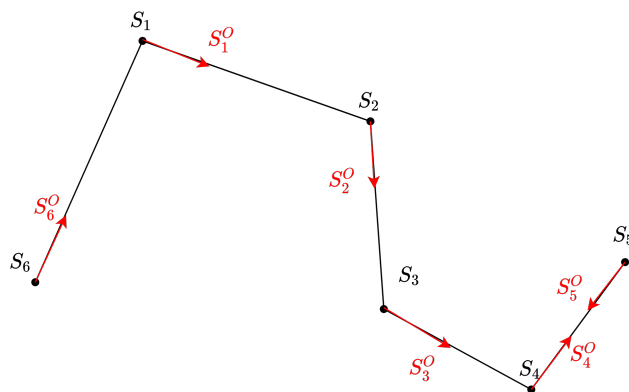


Fig. 7. Resulting offspring individuals $\{S_i^O\}_{i=1}^6$ (in red) generated from the population $\{S_i\}_{i=1}^6$ (in black).

The overall parent matching and the AUX crossover are summarized in Algorithm 5. All the p crossover operations are performed in parallel on individual GPU threads.

3.6 MPMA implementation on graphic processing units

MPMA was programmed in Python with the Numba library for CUDA kernel implementation. It is specifically designed to run on GPUs. In this work we used a V100 Nvidia graphic card with 32 GB memory.

Figure 8 shows the organization of the threads on the GPU grid and the memory hierarchy on the GPUs used to run the p tabu searches in parallel for the whole population at each generation. Each of the p tabu searches (cf. Section 3.3) is run on a single thread. For fast memory access, a per-thread local memory is used to store specific local information such as the current solution being ameliorated and the tabu tenure. The threads are grouped by block of size 64 and launched on the GPU grid. No per-block shared memory is used because all the local searches performed in each block are independent from each other. However, a global memory is employed to store general information about the graph such as its adjacency matrix of the graph and the color domain of each vertex to avoid information duplication. All these p tabu searches are launched

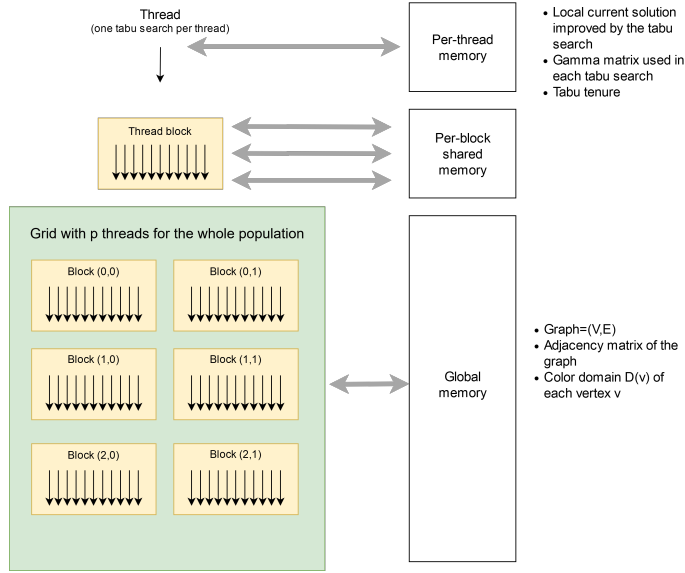


Fig. 8. Parallel tabu searches launched on GPU grid.

with a CUDA kernel function and the best results obtained during each tabu search are transferred to the CPU after synchronization.

The same type of kernel function on the GPUs is used to compute in parallel the $p \times p + p \times (p - 1)/2$ distance calculations (cf. Section 3.4) and the p crossovers (cf. Section 3.5) at each generation. However, some operations such as the best solution saving procedure and the population update procedure (cf. Section 3.4) are performed on the CPU as they cannot be parallelized.

3.7 A variant of the algorithm for highly constrained instances

As shown in Section 4, the MPMA algorithm excels on under-constrained to moderately over-constrained PLSE instances with a filled ratio r below 80%. However, its performance slightly deteriorates on highly constrained instances when $r \geq 80\%$. For these cases, we observed that better results can be reached by directly minimizing the number of uncolored vertices (i.e., fitness $f(\cdot)$ of Section 2.1) in the space of legal (i.e., conflict-free) partial colorings. For these highly constrained instances, we create a simplified MPMA variant called Partial-MPMA that works with legal partial colorings (instead of conflicting colorings) and makes the following two changes in MPMA.

- A greedy conflict removal procedure is applied to repair each offspring solution into a legal partial coloring. For this, the vertex which is conflicting with the largest number of vertices is uncolored first (i.e., reassigned the color 0), followed by the vertex with the second largest conflicts and so on.

This process continues until a partial conflict-free coloring is reached.

- The two-phase tabu search procedure of Section 3.3 is replaced by the PartialCol coloring algorithm of [33] adapted to the list-coloring problem. This PartialCol algorithm uses tabu search to explore the space of legal partial colorings by minimizing the number of uncolored vertices.

4 Experimental results

This section is dedicated to a computational assessment of the MPMA algorithm for solving the partial Latin square extension problem, by making comparisons with the state-of-the-art methods. Additional results are presented in Appendix B for the related Latin square completion problem.

4.1 Benchmark instances

We carried out extensive experiments on the 1800 PLSE benchmark instances introduced in [12]. These instances are parametrized by the grid order $n \in \{50, 60, 70\}$ and the ratio $r \in \{0.3, 0.4, \dots, 0.8\}$ of pre-filled cells in the $n \times n$ grid. Given (n, r) and starting from an empty $n \times n$ grid, a PLSE instance was constructed by repeatedly assigning a different symbol in an empty cell chosen randomly so that the Latin square condition is respected and until $r \times n^2$ cells are assigned symbols. For each (n, r) combination, 100 instances are available. Note that such a PLSE instance does not always admit a complete solution (i.e., some cells must be left unfilled). This is typically the case for relatively strongly constrained instances when $r > 60$ (i.e., when at least 60% cells are pre-filled). Moreover, as shown in [9,12], under-constrained instances ($r \leq 0.5$) and over-constrained instances ($r > 0.7$) are easier than medium-constrained instances with r between 0.6 and 0.7.

It is clear that n^2 is an upper bound for these instances (all cells are filled). When the grid cannot be fully filled, a safe upper bound is given in [18], corresponding to $n^2 - 2$ (all but 2 cells are filled). This bound indicates that if a grid cannot be completed, at least two cells will be left unfilled.

Like [14], we first convert these instances to Latin square graphs and apply the preprocessing algorithm of Section 2.2 to reduce them, leading to graphs with less than 500 vertices for $(n, r) = (50, 0.8)$ and up to 3430 vertices for $(n, r) = (70, 0.3)$. The preprocessing takes no more than several seconds.

4.2 Parameter setting

The population size p of MPMA is set to $p = 12288$, which is chosen as a multiple of the number of 64 threads per block. This large population size offers a good performance ratio on the Nvidia V100 graphics card that we used in our experiments, while remaining reasonable for pairwise distance calculations in the population, as well as the memory occupation on the GPU, especially when solving very large instances. A sensitivity experiment of the results with respect to the population size is presented in Section 5. In addition to the population size, the parameter α of the tabu search is set to its classical value of 0.6 and the number of tabu iterations $nbIter_{TS}$ depends on the size $|V|$ of the graph. The parameter γ for the minimum spacing between two individuals is set to 10. The parameter β for adjusting the distance of the offspring from their parents is fixed at 20.

Table 1 summarizes the parameter setting, which can be considered as the default and is used for all our experiments.

Table 1

Parameter setting in MPMA

Parameter	Description	Value
p	Population size	12288
$nbIter_{TS}$	Number of iterations tabu search	$100 \times V $
α	Tabu tenure parameter	0.6
γ	Parameter for the spacing between two individuals	10
β	Parameter for the generation of offspring	20

4.3 Comparative results on the set of 1800 PLSE instances

This section shows a comparative analysis on the 1800 PLSE instances with respect to the state-of-the-art methods. Given the stochastic nature of the MPMA algorithm, each instance is independently solved 5 times.

Table 2 summarizes the computational results of MPMA compared to the best results in the literature reported in [12,14]. For each instance MPMA was launched with a maximum of 100 billions of tabu search iterations. The reference methods include the 7 PLSE approaches in [12]: CPX-IP, CPX-CP, LSSOL, 1-ILS*, 2-ILS, 3-ILS and Tr-ILS*, where CPX-IP and CPX-CP are exact Integer Programming and Constraint Programming solvers from IBM/ILOG CPLEX, LSSOL denotes the tool LocalSolver. 1-ILS*, 2-ILS, 3-ILS and Tr-ILS* are four iterated local search algorithms with three different neighborhoods. We also cite the results of the recent MMCOL algorithm [14], which is designed for the related LSC problem and reported results on the 1800 PLSE instances with an adapted version of MMCOL.

Table 2

Comparative results of MPMA and its Partial-MPMA variant with the state-of-the-art methods (CPX-IP, CPX-CP, LSSOL, 1-ILS*, 2-ILS, 3-ILS, Tr-ILS* in [12] and MMCOL in [14]) in terms of the average number of filled cells for each type of 100 PLSE instances of size $n \in \{50, 60, 70\}$ and ratio of pre-assigned symbols $r \in \{0.3, 0.4, 0.5, 0.6, 0.7, 0.8\}$. Dominating results are indicated in bold.

Instance		CPX-IP	CPX-CP	LSSOL	1-ILS*	2-ILS	3-ILS	Tr-ILS*	MMCOL	MPMA	Partial-MPMA
n	r	f_{best}	f_{best}	f_{best}	f_{best}	f_{best}	f_{best}	f_{best}	f_{best}	f_{best}	f_{best}
50	0.3	2496.03	2499.87	2496.35	2500*	2499.98	2499.96	2500*	2500*	2500*	2500*
	0.4	2493.78	2498.02	2494.65	2499.98	2500*	2499.86	2500*	2500*	2500*	2493.35
	0.5	2488.52	2489.92	2492.96	2499.89	2499.95	2499.25	2500*	2500*	2500*	2491.82
	0.6	2476.21	2478.87	2489.21	2496.23	2496.3	2494.67	2497.18	2499.64	2499.7	2485.64
	0.7	2446.4	2451.04	2463.45	2469.47	2469.78	2467.77	2470.07	2478.94	2484.38	2466.95
	0.8	2394.58	2388.1	2393.67	2394.14	2394.11	2394.09	2394.14	2364.61	2393.24	2394.58
	0.3	3593.07	3598.29	3593.2	3599.98	3600*	3599.28	3600*	3600*	3600*	3597.56
	0.4	3590.68	3592.55	3591.17	3599.97	3599.96	3598.58	3600*	3600	3600*	3596.2
60	0.5	3585.29	3585.83	3587.5	3599.65	3599.58	3597.53	3599.94	3600*	3600*	3589.18
	0.6	3572.61	3573.7	3585.52	3595.82	3595.85	3592.77	3596.67	3599.94	3599.94	3578.9
	0.7	3534.71	3540.45	3561.05	3571.47	3570.58	3566.51	3572.12	3589.82	3593.52	3556.65
	0.8	3478.58	3464.14	3476.44	3478.59	3478.37	3478.05	3478.49	3431.85	3477.80	3480.03
	0.3	4890.2	4893.75	4890.25	4899.98	4899.98	4897.32	4900*	4900*	4900*	4896.48
	0.4	4887.73	4888.36	4887.98	4899.96	4899.98	4896.4	4899.98	4900*	4900*	4887.62
	0.5	4881.09	4881.17	4882.9	4899.41	4899.44	4893.97	4899.57	4900*	4900*	4883.67
	0.6	4868.21	4868.74	4877.77	4895.3	4894.93	4888.52	4896.19	4900*	4900*	4874.82
70	0.7	4829.65	4831.94	4859.71	4872.41	4870.97	4864.38	4872.95	4894.58	4896.33	4848.31
	0.8	4761.44	4737.73	4761.17	4766.67	4765.81	4763.93	4765.91	4698.78	4766.33	4768.13

Columns 1 and 2 of Table 2 show the characteristics of each instance (i.e., grid order n and ratio r of pre-assigned symbols). Columns 3-10 present the average number of filled cells in the best solutions obtained by the reference algorithms for the 100 instances of each type (n, r) . The results of the proposed MPMA algorithm and Partial-MPMA variant are reported in columns 11 and 12 respectively¹. Bold numbers show the dominating values while a star indicates an optimal value (corresponding to the n^2 upper bound).

We observe that MPMA always obtain the best scores (in bold) except for the over-constrained instances with $r = 0.8$. For the instances with $r = 0.8$, the Partial-MPMA variant always obtain the best results.

The best competitors, Tr-ILS* and MMCOL, were launched with a limited amount of available times in [12,14]: up to 10 seconds for Tr-ILS* and up to two hours for MMCOL. In order to verify if these algorithms can improve their results by using more computation time, we ran the codes of these two best performing algorithms, with a much relaxed time limit of 48 hours. The results are shown in Table 3. For each compared algorithm, we report the best and average results over 5 runs (f_{best} and f_{avg}) as well as the average computation time needed to reach its best result.

With this much relaxed time limit, both Tr-ILS* and MMCOL indeed improve their-own results reported in [12] and [14] (also shown in Table 2). Meanwhile, MMCOL and Tr-ILS* are still outperformed by MPMA/Partial-MPMA on the strongly constrained instances with $r \geq 0.7$.

For under-constrained (easy) instances, one notices that MPMA takes much more times to achieve its best results. This comes from the fact that every kernel operation launched on the GPU cannot be stopped until it is completed on each thread. Therefore, even if a solution of the instance is found in one thread, one still needs to wait for all the threads to finish their computation before retrieving the result. In fact, for these easy instances, a very large population with a high diversity is not really mandatory. MPMA can reach the optimal solutions faster with a much reduced population.

On the other hand, using a very large population with a high diversity becomes critical when dealing with the most difficult instances such as those with $r \geq 0.7$. For these instances, MPMA obtains equal or better results compared to Tr-ILS* and MMCOL for all orders $n = 50, 60, 70$. Detailed results for the very difficult instances with $r = 0.7$ are displayed in Appendix A (Table A.1). Moreover, MPMA can optimally solve 25 of the 100 most challenging instances with $n = 70$ and $r = 0.7$ (cf. Table A.1).

¹ The certificates of the best solutions of MPMA and Partial-MPMA for these 1800 instances are available at <https://github.com/GoudetOlivier/MPMA>

Table 3

Comparison of MPMA/Partial-MPMA with MMCOL [14] and Tr-ILS* [12] with a much relaxed time limit of 48h on the PLSE instances.

Instance		Tr-ILS* (ext. time)			MMCOL (ext. time)			MPMA/Partial-MPMA		
n	r	f_{best}	f_{avg}	t(s)	f_{best}	f_{avg}	t(s)	f_{best}	f_{avg}	t(s)
50	0.3	2500*	2500	1	2500*	2500	0.22	2500*	2500	142
	0.4	2500*	2500	2	2500*	2500	0.16	2500*	2500	112
	0.5	2500*	2500	2	2500*	2500	0.31	2500*	2500	89
	0.6	2499.63	2498.94	152	2499.7	2499.7	17.55	2499.7	2499.7	489
	0.7	2473.53	2472.84	511	2479.13	2478.48	46996	2484.38	2483.99	24970
	0.8	2394.34	2393.65	658	2378.15	2377.50	16268	2394.58	2394.42	3916
	60	0.3	3600*	3600	2	3600*	3600	0.69	3600*	3600
0.4		3600*	3600	2	3600*	3600	0.52	3600*	3600	298
0.5		3600*	3600	17	3600*	3600	0.67	3600*	3600	214
0.6		3599.94	3599.25	69	3599.94	3599.94	13.41	3599.94	3599.94	759
0.7		3576.7	3576.01	1388	3590.22	3589.56	49279	3593.52	3593.13	35658
0.8		3478.92	3478.23	460	3457.07	3456.42	77979	3480.05	3479.94	18141
70		0.3	4900*	4900	3	4900*	4900	0.90	4900*	4900
	0.4	4900*	4900	2	4900*	4900	0.65	4900*	4900	489
	0.5	4899.71	4899.22	18	4900*	4900	1.51	4900*	4900	349
	0.6	4899.98	4899.30	437	4900*	4900	19.82	4900*	4900	1210
	0.7	4880.10	4879.31	3245	4895.21	4894.54	55887	4896.33	4895.93	46746
	0.8	4767.24	4766.33	2145	4736.70	4736.07	120862	4768.13	4767.93	56670

It is difficult to compare the computation time between MPMA and the competitors, as MPMA uses a GPU while the other algorithms use a CPU. Therefore we compare MPMA and MMCOL in terms of number of iterations in order to observe whether the best results of MPMA come from the algorithm itself or from the parallelization. As both MPMA and MMCOL use a one-move tabu search, the number of local search iterations is suitable comparison criterion. We run MPMA and MMCOL with a maximum of 100 billions iterations of tabu search on the first ten instances of each of the most difficult (n, r) combinations with $n = 50, 60, 70$ and $r = 70, 80$. Each instance is independently solved 5 times. The detailed results are reported in Table 4, where we show for each instance and each algorithm (MMCOL, MPMA), the best result f_{best} over the 5 trials, the average result f_{avg} over these 5 trials, the average computation time in hours $t(h)$ required to reach the best result and the average number of local search iterations nb_iter required to reach the best score. The best results are indicated in bold. According to the results, MPMA can achieve better or equal results for all instances with the same overall number of iterations. In addition, the use of a GPU reduces the time spent by the algorithm, because this important number of iterations can be performed in a shorter amount of time thanks to parallelization. This experiment confirms that the proposed MPMA algorithm dominates MMCOL.

Table 4
 Comparison of MPMA with MMCOL [14] with a large number of iterations on the PLSE instances (maximum of 100×10^9 iterations).

Instance	MMCOL (ext. nb iter.)			MPMA			Instance	MMCOL (ext. nb iter)			MPMA					
	f_{best}	f_{avg}	t(h)	nb_iter.	f_{best}	f_{avg}		t(h)	nb_iter	f_{best}	f_{avg}	t(h)	nb_iter			
QC-50-70-1	2479	2478.2	168	82×10^9	2485	2484.0	4	36×10^9	2380	2379.6	38	14×10^9	2393	2392.8	0.2	3×10^9
QC-50-70-2	2477	2476.6	45	24×10^9	2482	2482.0	2	20×10^9	2377	2376.4	18	9×10^9	2391	2391	0.03	0.5×10^9
QC-50-70-3	2487	2486.6	150	81×10^9	2490	2489.6	5	44×10^9	2381	2380.2	3	1×10^9	2395	2395	0.5	7×10^9
QC-50-70-4	2482	2481	54	29×10^9	2487	2486.8	3	28×10^9	2386	2385.6	15	6×10^9	2399	2399	0.03	0.5×10^9
QC-50-70-5	2474	2474	139	68×10^9	2482	2481.6	10	94×10^9	2377	2376.4	15	6×10^9	2388	2388	1.5	27×10^9
QC-50-70-6	2481	2480.2	28	14×10^9	2485	2484.6	5	44×10^9	2378	2377.8	5	2×10^9	2393	2393	2	34×10^9
QC-50-70-7	2480	2479.6	186	92×10^9	2485	2485.0	6	57×10^9	2387	2387	121	44×10^9	2404	2403.8	0.2	3×10^9
QC-50-70-8	2476	2475.4	98	49×10^9	2483	2482.6	6	62×10^9	2367	2366.4	38	14×10^9	2389	2389	0.4	6×10^9
QC-50-70-9	2483	2482.4	45	24×10^9	2486	2485.8	8	84×10^9	2378	2377.2	2	2×10^9	2393	2393	0.2	4×10^9
QC-50-70-10	2472	2471.4	26	10×10^9	2480	2479.6	9	75×10^9	2362	2361	45	11×10^9	2382	2382	0.03	0.5×10^9
QC-60-70-1	3593	3592.8	121	51×10^9	3594	3593.8	6	39×10^9	3448	3449.2	147	27×10^9	3467	3467	0.2	2×10^9
QC-60-70-2	3590	3589.4	71	36×10^9	3594	3593.2	9	59×10^9	3453	3452.2	88	20×10^9	3472	3472	3	22×10^9
QC-60-70-3	3578	3577.2	160	55×10^9	3583	3582.4	14	91×10^9	3454	3452.6	50	11×10^9	3475	3474.8	2	21×10^9
QC-60-70-4	3592	3591	164	58×10^9	3595	3595	11	72×10^9	3464	3463.2	50	10×10^9	3482	3482	1	10×10^9
QC-60-70-5	3592	3591.2	267	94×10^9	3594	3593.8	7	42×10^9	3471	3470.4	73	15×10^9	3490	3489.6	3	40×10^9
QC-60-70-6	3596	3595	287	99×10^9	3598	3597.0	10	64×10^9	3450	3448	233	45×10^9	3476	3476	0.5	5×10^9
QC-60-70-7	3589	3588	162	57×10^9	3591	3590.8	8	52×10^9	3459	3458.4	75	31×10^9	3478	3478	1.5	16×10^9
QC-60-70-8	3590	3589.2	241	85×10^9	3593	3592.6	9	59×10^9	3464	3462.8	49	24×10^9	3488	3488	0.3	3×10^9
QC-60-70-9	3592	3592	94	36×10^9	3595	3594.4	13	85×10^9	3448	3447.6	53	18×10^9	3471	3471	1.5	16×10^9
QC-60-70-10	3590	3589.2	235	65×10^9	3592	3591.4	8	51×10^9	3457	3456.6	88	26×10^9	3477	3477	1.4	15×10^9
QC-70-70-1	4895	4894.8	47	15×10^9	4897	4897.0	18	84×10^9	4729	4727.2	59	9×10^9	4766	4764.8	2	16×10^9
QC-70-70-2	4895	4895	151	51×10^9	4896	4896.0	9	42×10^9	4738	4736.4	23	4×10^9	4771	4768.6	4	33×10^9
QC-70-70-3	4897	4896.6	125	48×10^9	4897	4897.0	11	51×10^9	4721	4720.4	22	3×10^9	4756	4755	4	28×10^9
QC-70-70-4	4893	4892.4	69	27×10^9	4894	4893.8	17	79×10^9	4735	4733.4	124	22×10^9	4770	4767.8	2	17×10^9
QC-70-70-5	4898	4898	177	91×10^9	4898	4897.6	8	38×10^9	4748	4745.8	174	32×10^9	4768	4768	2	19×10^9
QC-70-70-6	4900	4898.6	63	29×10^9	4900	4899.2	7	32×10^9	4747	4746.2	82	14×10^9	4773	4772.8	3	24×10^9
QC-70-70-7	4898	4897.8	146	71×10^9	4898	4897.6	19	89×10^9	4746	4744	19	3×10^9	4774	4774	1	9×10^9
QC-70-70-8	4897	4896.6	189	92×10^9	4898	4898	9	43×10^9	4745	4744.2	57	8×10^9	4777	4775	2	15×10^9
QC-70-70-9	4897	4896.2	85	52×10^9	4898	4896.8	16	81×10^9	4730	4728.8	8	1×10^9	4761	4760.4	2	15×10^9
QC-70-70-10	4897	4896.4	93	46×10^9	4897	4896.8	7	31×10^9	4750	4748.8	60	9×10^9	4777	4776	4	28×10^9

In summary, MPMA and its Partial-MPMA variant for highly constrained instances (when $r > 0.7$) compete very favorably with the best performing PLSE methods in the literature, by reporting equal or better results on the 1800 benchmark instances. In Appendix B, we show that MPMA also performs extremely well on the special case of the Latin square completion problem, by attaining the optimal solutions for all the LSC benchmark instances.

5 Analysis of important factors in the algorithm

In this section, we analyze the impacts of three important factors of the MPMA algorithm: (i) its very large population, the AUX crossover and (iii) the nearest neighbor matching strategy for parent selection. These experiments are based on the first ten hard instances with $n = 60$ and $r = 0.7$ of the PLSE.

5.1 Sensitivity to the population size

We first perform a sensitivity analysis of the algorithm with respect to the population size. For this, we perform the MPMA algorithm with p varying in the range $[10, 12288]$ to solve each of the ten instance 5 times under a time limit to 20 hours per run. Figure 9 displays the sensitivity of the average results to the population size p .

For the same time budget, the MPMA algorithm obtains better results with a larger size. When $p = 12288$, the algorithm always attains the best score over 10 runs. This can be explained by two reasons. First, due to the parallelization of the calculations on the GPUs, a large population improves the diversity of the population and helps the algorithm to perform a higher average global number of iterations at each run, which in turn increases the chance to attain high-quality solutions. Second, a large population increases the chance for each individual to find a closer but different nearest neighbor in the population for parent matching of the AUX crossover, which helps to generate promising offspring solutions.

5.2 Impact of the asymmetric uniform crossover

To study the impact of the asymmetric uniform crossover AUX on the MPMA algorithm, we compare it with four different variants of MPMA where the AUX crossover described in Section 3.5.2 is changed or disabled.

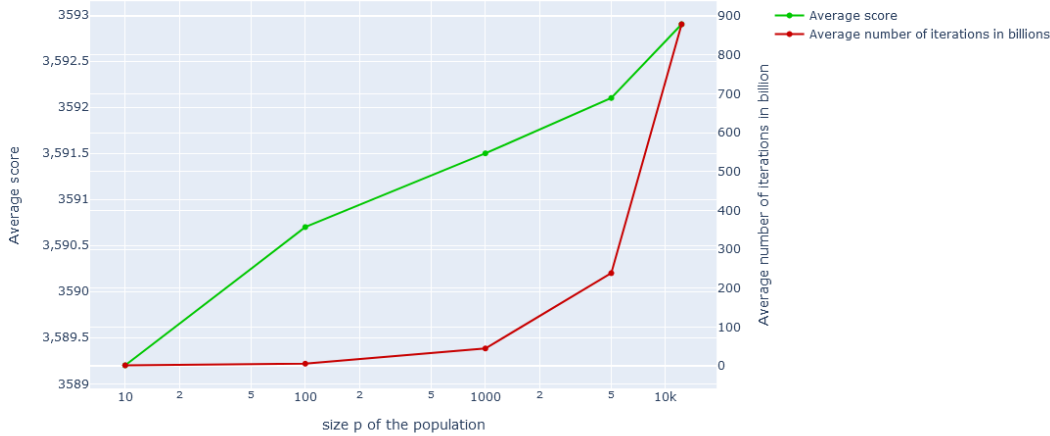


Fig. 9. Impact of the population size p on the performance of MPMA. Green curve corresponds to the average score and red curve to the average number of iterations in billions required to reach the best scores.

- The first variant is a baseline variant without crossover, so each offspring is an exact copy of its first parent.
- The greedy partition crossover GPX [30] is adapted for the Latin square problem: each color class of the offspring inherits the largest color class of the selected parent.
- The AUX crossover is replaced by the maximum approximate group based crossover MAGX of the MMCOL algorithm for the related Latin square completion problem [14].
- The AUX crossover is replaced by the uniform crossover (UX) which corresponds to AUX with p_{ij} being fixed to the value of 0.5.

Figure 10 shows the evolution of the best fitness values averaged over 5 runs for the same ten PLSE instances with $(n, r) = (60, 0.7)$ through the number of generations of each algorithm. One notices that the crossovers GPX and UX, which are the most disruptive, perform badly and are even outperformed by the variant without crossovers (blue line). This can be explained by the fact that the individuals are very distant in the population and rarely share large common features. Indeed, we experimentally observed that the average pairwise distance in the population is usually very large, around $0.7 \times |V|$.

The AUX and MAGX crossovers perform the best and dominate GPX and UX. Meanwhile, AUX dominates MAGX after 50 generations in average. The difference is statistically significant (confirmed by t-test with the p-value of 0.001). One reason to explain the advantage of AUX over MAGX is that with the AUX crossover, the offspring inherits more features from one parent than from the other parent. On the contrary, since MAGX is a symmetric crossover, crossing-over (S_i, S_j) and (S_j, S_i) lead to the same offspring, which results in less diversified offspring in the next generation.

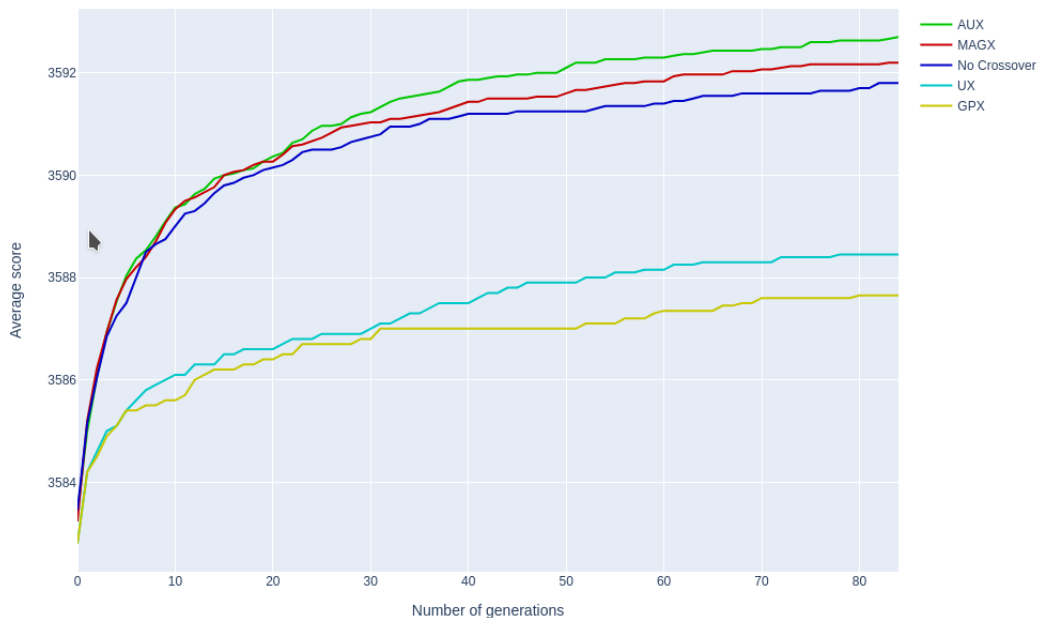


Fig. 10. Comparison of five different MPMA variants: No crossover (blue), GPX (yellow), MAGX (red), UX (light blue), AUX (green).

5.3 Impact of the crossover matching strategy

To study the impact of the nearest neighbor matching strategy for the AUX crossover, we run a MPMA variant where this matching strategy is replaced by a random matching strategy: each individual as the first parent is cross-overed with another individual chosen randomly in the population.

Figure 11 shows the evolution of the best fitness values averaged over 5 runs for the same 10 first PLSE instances with $(n, r) = (60, 0.7)$ with respect to the number of generations of the algorithm. One notices that the matching strategy has an important impact on the performance. The dominance of the nearest neighbor matching strategy over the random matching becomes more and more evident after 10 generations. The difference is statistically significant (t-test with the p-value of 0.001). This is because two parents chosen randomly in the very large population share little information, leading to poor offspring whose quality can be hardly raised even after local optimization. The nearest neighbor strategy avoids this problem, as it does not destroy too much the color classes transmitted to the offspring, while preserving a certain level of diversity. This creates opportunities for the subsequent local search to explore new and interesting areas of the search space.

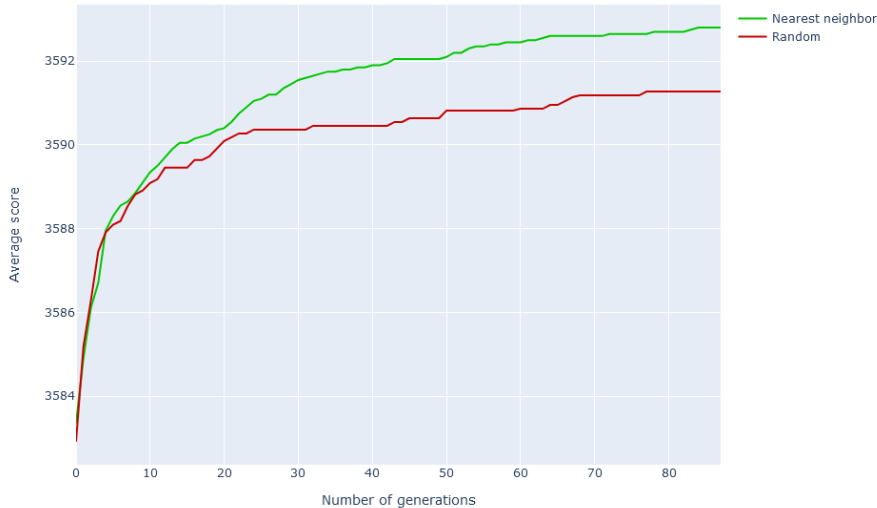


Fig. 11. Comparison of two parent matching strategies in MPMA: random matching (red) and nearest neighbor matching (green).

6 Conclusion

We presented a massively parallel population-based algorithm with a very large population and a practical implementation on GPUs to solve the partial Latin square extension problem as well as the special case of the Latin square completion problem. This approach highlights the interest of a very large population that enables massively parallel local optimization, offspring generations and distance calculations. The algorithm features a parameterized asymmetric crossover equipped with a dedicated parent matching strategy to build promising offspring, an effective parallel two-phase tabu search to improve new solutions and an original pool updating mechanism.

We performed extensive experiments to assess the proposed algorithm on the set of 1800 benchmark instances with various orders and ratios of pre-filled cells. The results showed that the algorithm obtains state-of-the-art results in average for all Latin square configurations (n, r) . Furthermore, it definitely closed 25 challenging instances of order $n = 70$ and ratio $r = 0.7$. We investigated the impacts of key algorithmic components including the large population size and the parent matching strategy. This work demonstrates for the first time the high potential of GPU-based parallel computations for solving the challenging Latin square extension problem, by exploiting the formidable computing power offered by the GPUs and designing suitable search strategies.

The proposed algorithm can be used to solve relevant problems related to the PLSE. The availability of the source code of our algorithm will facilitate such applications. The design ideas of the algorithm can help to develop effective algorithms for other difficult combinatorial optimization problems. Future

works could be carried out in particular to improve the parent matching strategy. For instance, it would be interesting to investigate strategies driven by a deep graph convolutional neural network in order to build the most promising offspring from appropriate parents.

CRedit author statement

Olivier Goudet: Conceptualization, Methodology, Software, Investigation, Writing - Original Draft. **Jin-Kao Hao:** Conceptualization, Methodology, Investigation, Writing - Original Draft.

Acknowledgment

We would like to thank Dr. Kazuya Haraguchi for sharing his Tr-ILS* code and the instances [12]. We are grateful to Dr. Yan Jin for her assistance on their MMCOL code [14]. This work was granted access to the HPC resources of IDRIS (Grant No. 2020-A0090611887) from GENCI.

References

- [1] A. D. Keedwell, J. Dénes, Latin Squares and their Applications, Elsevier North Holland, 2015.
- [2] D. Jakobovic, S. Picek, M. S. Martins, M. Wagner, Toward more efficient heuristic construction of boolean functions, *Applied Soft Computing* 107 (2021) 107327.
- [3] R. A. Barry, P. A. Humblet, Latin routers, design and implementation, *Journal of Lightwave Technology* 11 (5/6) (1993) 891–899.
- [4] C. J. Colbourn, The complexity of completing partial latin squares, *Discrete Applied Mathematics* 8 (1) (1984) 25–30.
- [5] T. Evans, Embedding incomplete latin squares, *The American Mathematical Monthly* 67 (10) (1960) 958–961.
- [6] F. E. Bennett, Quasigroup identities and mendelsohn designs, *Canadian Journal of Mathematics* 41 (2) (1989) 341–368.
- [7] V. A. Artamonov, S. Chakrabarti, S. K. Pal, Characterization of polynomially complete quasigroups based on latin squares for cryptographic transformations, *Discrete Applied Mathematics* 200 (2016) 5–17.

- [8] V. A. Artamonov, S. Chakrabarti, S. Gangopadhyay, S. Pal, On latin squares of polynomially complete quasigroups and quasigroups generated by shifts, *Quasigroups and Related Systems* 21 (2) (2013) 117–130.
- [9] C. Gomes, D. Shmoys, Completing quasigroups or latin squares: A structured graph coloring problem, in: *Proceedings of the Computational Symposium on Graph Coloring and Generalizations*, 2002, pp. 22–39.
- [10] C. Ansótegui, A. del Val, I. Dotú, C. Fernández, F. Manyà, Modeling choices in quasigroup completion: SAT vs. CSP, in: *Proceedings of the 19th AAAI*, AAAI Press, 2004, pp. 137–142.
- [11] C. P. Gomes, R. G. Regis, D. B. Shmoys, An improved approximation algorithm for the partial latin square extension problem, *Operations Research Letters* 32 (5) (2004) 479–484.
- [12] K. Haraguchi, Iterated local search with trellis-neighborhood for the partial latin square extension problem, *Journal of Heuristics* 22 (5) (2016) 727–757.
- [13] R. Lewis, *A guide to graph colouring*, Springer, 2015.
- [14] Y. Jin, J.-K. Hao, Solving the latin square completion problem by memetic graph coloring, *IEEE Transactions on Evolutionary Computation* 23 (6) (2019) 1015–1028.
- [15] R. Banos, C. Gil, J. Reca, F. G. Montoya, A memetic algorithm applied to the design of water distribution networks, *Applied Soft Computing* 10 (1) (2010) 261–266.
- [16] L. G. B. Ruíz, M. I. Capel, M. Pegalajar, Parallel memetic algorithm for training recurrent neural networks for the energy efficiency problem, *Applied Soft Computing* 76 (2019) 356–368.
- [17] Z. Lü, J.-K. Hao, A memetic algorithm for graph coloring, *European Journal of Operational Research* 203 (1) (2010) 241–250.
- [18] D. Donovan, The completion of partial latin squares, *Australasian Journal of Combinatorics* 22 (2000) 247–264.
- [19] D. C. Porumbel, J.-K. Hao, P. Kuntz, An efficient algorithm for computing the distance between close partitions, *Discrete Applied Mathematics* 159 (1) (2011) 53–59.
- [20] J.-K. Hao, Memetic algorithms in discrete optimization, in: *Handbook of Memetic Algorithms*, Springer, 2012, pp. 73–94.
- [21] L. Moalic, A. Gondran, Variations on memetic algorithms for graph coloring problems, *Journal of Heuristics* 24 (1) (2018) 1–24.
- [22] Y. Chen, J.-K. Hao, F. Glover, A hybrid metaheuristic approach for the capacitated arc routing problem, *European Journal of Operational Research* 253 (1) (2016) 25–39.

- [23] X. Lai, J.-K. Hao, F. Glover, Z. Lü, A two-phase tabu-evolutionary algorithm for the 0–1 multidimensional knapsack problem, *Information Sciences* 436 (2018) 282–301.
- [24] W. Sun, J.-K. Hao, X. Lai, Q. Wu, Adaptive feasible and infeasible tabu search for weighted vertex coloring, *Information Sciences* 466 (2018) 203–219.
- [25] F. Neri, C. Cotta, P. Moscato (Eds.), *Handbook of Memetic Algorithms*, Vol. 379 of *Studies in Computational Intelligence*, Springer, 2012.
- [26] Y. Jin, J.-K. Hao, J.-P. Hamiez, A memetic algorithm for the minimum sum coloring problem, *Computers & Operations Research* 43 (2014) 318–327.
- [27] W. Sun, J.-K. Hao, W. Wang, Q. Wu, Memetic search for the equitable coloring problem, *Knowledge-Based Systems* 188 (2020) 105000.
- [28] A. Hertz, D. de Werra, Using tabu search techniques for graph coloring, *Computing* 39 (4) (1987) 345–351.
- [29] W. Wang, J.-K. Hao, Q. Wu, Tabu search with feasible and infeasible searches for equitable coloring, *Engineering Applications of Artificial Intelligence* 71 (2018) 1–14.
- [30] P. Galinier, J.-K. Hao, Hybrid evolutionary algorithms for graph coloring, *Journal of Combinatorial Optimization* 3 (4) (1999) 379–397.
- [31] E. Malaguti, M. Monaci, P. Toth, A metaheuristic approach for the vertex coloring problem, *INFORMS Journal on Computing* 20 (2) (2008) 302–316.
- [32] G. Syswerda, Uniform crossover in genetic algorithms, in: J. D. Schaffer (Ed.), *Proceedings of the 3rd International Conference on Genetic Algorithms*, George Mason University, Fairfax, Virginia, USA, June 1989, Morgan Kaufmann, 1989, pp. 2–9.
- [33] I. Blöchliger, N. Zufferey, A graph coloring heuristic using partial solutions and a reactive tabu scheme, *Computers & Operations Research* 35 (3) (2008) 960–975.

A Detailed results for the challenging PLSE instances with $r = 0.7$

According to [12], instances with $r = 0.7$ are among the most challenging. Table A.1 present the detailed results obtained by the MPMA algorithm on the three sets of 300 PLSE instance with $r = 0.7$ and $n = 50, 60, 70$. Column 1 identifies the instances of each type (n, r) . For each instance, we report the best PLSE score f_{best} (i.e., the largest number of filled cells) obtained over 5 runs with a maximum of 100 billions of tabu iterations, average score f_{avg} and average computation time $t(s)$ in seconds to reach the best results. Bold

values are the record-breaking results compared to the best-known results in the literature (including the best results obtained by running the codes of Tr-ILS* [12] and MMCOL [14] with the extended time limit of 48h). A star indicates an optimal value. The optimality is proved if (i) the number of filled cells reaches the upper bound $n^2 - l$ if $l \neq 1$ (cf. Section 2.2), or (ii) the number of filled cells is $n^2 - 2$ if $l = 1$ (cf. Theorem 6 in [18]). One observes that MPMA improves the best-known results for a large majority of the 300 instances and closes definitively 25 instances by reaching their optimal scores. Among these 25 optimal results, 14 were also achieved by MMCOL (starred non-bold values) with the extended time limit.

Table A.1
Detailed results of MPMA for the PLSE instance with $r = 0.7$

Id	PLSE-50-70			PLSE-60-70			PLSE-70-70		
	f_{best}	f_{avg}	t(s)	f_{best}	f_{avg}	t(s)	f_{best}	f_{avg}	t(s)
1	2485	2484.0	14634	3594	3593.8	21133	4897	4897.0	64501
2	2482	2482.0	7979	3594	3593.2	32775	4896	4896.0	31215
3	2490	2489.6	16640	3583	3582.4	50463	4897	4897.0	38822
4	2487	2486.8	11040	3595	3595.0	42003	4894	4893.8	60959
5	2482	2481.6	38581	3594	3593.8	23419	4898*	4897.6	29179
6	2485	2484.6	17336	3598	3597.0	35415	4900*	4899.2	24546
7	2485	2485.0	21093	3591	3590.8	29223	4898*	4897.6	68794
8	2483	2482.6	22696	3593	3592.6	31549	4898	4898.0	34353
9	2486	2485.8	29292	3595	3594.4	45923	4898*	4896.8	56775
10	2480	2479.6	33675	3592	3591.4	27668	4897	4896.8	24600
11	2488	2488.0	10494	3591	3591.0	43547	4895	4895.0	41911
12	2485	2484.8	11099	3595	3595.0	29279	4895	4895.0	49769
13	2483	2482.0	35398	3591	3590.6	30085	4896	4896.0	38843
14	2483	2483.0	24327	3596	3594.8	12871	4900*	4900.0	49655
15	2483	2483.0	22104	3598	3597.6	42935	4897*	4897.0	44162
16	2484	2484.0	24908	3589	3588.4	46321	4895	4894.4	51131
17	2486	2486.0	30868	3589	3588.2	44392	4898*	4897.8	55798
18	2489	2488.6	43310	3594	3594.0	31095	4896	4895.2	45508
19	2485	2485.0	46223	3592	3591.6	34286	4896	4895.0	33190
20	2490	2490.0	66822	3595	3595.0	45880	4898*	4898.0	45274
21	2483	2482.8	10055	3594	3593.8	28887	4896	4895.8	43046
22	2484	2483.8	31473	3594	3593.6	36060	4892	4891.8	51100
23	2485	2485.0	59471	3595	3594.8	35139	4898*	4897.4	57851
24	2488	2487.2	39261	3595	3594.2	39917	4896	4895.6	62074
25	2484	2484.0	67246	3595	3595.0	24632	4896	4895.6	29744
26	2483	2482.4	11660	3591	3590.4	29959	4896	4896.0	49052
27	2481	2480.8	17530	3596	3595.6	21738	4896	4895.2	64276
28	2484	2484.0	57286	3593	3592.2	39360	4895	4895.0	30988
29	2486	2486.0	24712	3594	3593.8	36996	4894	4893.0	33507
30	2485	2484.4	32252	3594	3593.2	29165	4894	4893.8	67407
31	2481	2480.2	30863	3596	3595.8	28915	4895	4894.8	66784
32	2481	2480.8	26209	3598	3597.8	36874	4898*	4898.0	63561
33	2483	2482.0	15300	3594	3593.8	50209	4893	4892.8	53578
34	2484	2483.6	17261	3595	3594.8	25322	4896	4896.0	29581
35	2483	2482.2	9258	3594	3593.6	48250	4895	4893.8	37046
36	2484	2483.8	39607	3589	3588.8	52302	4896	4896.0	30549
37	2486	2486.0	30891	3592	3591.8	36935	4898	4897.4	33335
38	2479	2479.0	27487	3593	3593.0	42965	4896	4895.8	46231
39	2482	2482.0	17885	3592	3592.0	40127	4895	4895.0	45687
40	2486	2485.8	25149	3584	3584.0	28671	4897	4897.0	39611
41	2486	2484.8	20498	3593	3593.0	44563	4894	4894.0	68759
42	2485	2484.2	29963	3596	3594.8	20232	4900*	4900.0	37155
43	2486	2485.6	22424	3592	3591.8	33863	4897	4896.4	65871
44	2478	2478.0	21238	3596	3595.2	39637	4900*	4900.0	24920
45	2487	2486.2	4387	3594	3593.2	53331	4896	4895.6	36570
46	2486	2485.2	8202	3590	3590.0	31509	4895	4894.4	66643
47	2483	2483.0	15598	3596	3596.0	50515	4896	4895.2	28201
48	2485	2485.0	12008	3594	3594.0	52813	4898*	4898.0	45563
49	2488	2487.8	19546	3592	3592.0	30852	4896	4896.0	61217
50	2487	2486.2	36084	3591	3590.4	28170	4892	4891.2	63410
51	2482	2482.0	14454	3597	3596.8	27863	4894	4893.2	52307
52	2483	2482.8	3734	3594	3593.2	29788	4894	4893.6	47142
53	2479	2478.2	29808	3590	3590.0	34304	4895	4895.0	61063
54	2482	2482.0	31105	3595	3595.0	36915	4895	4894.8	49282
55	2490	2490.0	57119	3593	3592.8	43977	4898	4898.0	42535
56	2486	2485.2	16890	3594	3594.0	26958	4897	4896.6	40521
57	2485	2484.0	17693	3596	3595.6	22850	4897	4895.8	36423
58	2484	2483.6	22020	3592	3590.8	42025	4895	4895.0	50358
59	2479	2479.0	17566	3597	3597.0	35690	4897	4896.2	48762
60	2485	2483.8	12812	3594	3594.0	49378	4898*	4897.6	41952
61	2488	2487.6	32457	3593	3593.0	34521	4896	4895.6	40522
62	2483	2482.2	11236	3595	3595.0	36297	4897	4896.6	26971
63	2484	2483.8	49638	3593	3593.0	33612	4895	4894.0	36138
64	2487	2486.8	18411	3589	3589.0	45479	4896	4895.8	43970
65	2483	2483.0	14955	3594	3592.8	51097	4895	4894.2	64374
66	2487	2486.0	6173	3594	3593.8	32932	4897	4895.8	29134
67	2492	2491.4	13935	3596	3594.8	46629	4896	4895.2	39470
68	2485	2484.6	13185	3591	3591.0	46103	4894	4893.6	65397
69	2480	2478.8	61028	3597	3596.8	29333	4896	4895.4	33751
70	2480	2480.0	10097	3596	3595.0	21332	4897	4896.4	70332
71	2485	2484.8	14403	3597	3596.8	26326	4898*	4896.8	37049
72	2485	2485.0	23233	3593	3593.0	41770	4898*	4897.6	55525
73	2481	2481.0	13541	3592	3591.8	42388	4897	4896.2	41423
74	2487	2486.2	17062	3591	3590.4	41805	4895	4894.8	66514
75	2486	2485.8	6442	3591	3589.8	37734	4893	4892.6	27458
76	2482	2481.6	31480	3596	3595.6	32075	4895	4894.4	37566
77	2484	2484.0	30772	3594	3593.6	30518	4898*	4897.8	71196
78	2485	2484.2	25027	3594	3593.8	37885	4894	4892.8	61918
79	2486	2485.4	11737	3592	3592.0	13140	4895	4894.8	55482
80	2486	2485.0	11477	3591	3590.6	17375	4895	4893.8	43852
81	2484	2483.6	25867	3594	3594.0	49588	4898	4898.0	34218
82	2486	2486.0	12979	3596	3595.2	49521	4896	4895.0	54607
83	2484	2483.8	45426	3591	3591.0	36875	4897	4896.8	53219
84	2482	2480.8	13416	3597	3596.8	39570	4896	4895.6	55558
85	2486	2485.2	18071	3591	3591.0	54486	4895	4894.2	51972
86	2484	2483.6	21323	3591	3590.8	32150	4896	4895.2	64547
87	2482	2481.8	7322	3597	3596.2	21235	4898	4897.8	58645
88	2486	2484.8	54905	3595	3594.0	31176	4898*	4897.6	55316
89	2483	2483.0	22200	3596	3595.2	42334	4898*	4898.0	69525
90	2484	2483.4	41303	3591	3590.6	28078	4898*	4897.8	33387
91	2485	2485.0	27282	3595	3594.8	37660	4898*	4897.8	35507
92	2480	2478.8	64358	3595	3595.0	20591	4898	4898.0	44032
93	2485	2484.6	54895	3595	3594.4	34376	4898*	4897.4	30656
94	2488	2487.4	36221	3593	3592.6	27382	4898*	4898.0	42838
95	2485	2484.2	34930	3596	3596.0	47333	4895	4894.0	15877
96	2484	2484.0	20119	3588	3587.4	26007	4898*	4897.2	56506
97	2483	2482.2	12874	3596	3594.8	18748	4895	4894.6	52890
98	2484	2483.6	17232	3595	3593.8	39620	4896	4895.8	34437
99	2487	2487.0	11038	3596	3595.0	44668	4900*	4900.0	48432
100	2481	2481.0	6466	3592	3591.6	38165	4895	4895.0	41758

B Results on the Latin square completion problem

The Latin square completion (LSC) problem can be considered as a special case of the partial Latin square extension problem. Two sets of LSC benchmark instances exist in the literature: 19 traditional instances [9] and 1800 new instances [12]. These instances were built from complete Latin squares with some symbols removed. Thus these instances have the optimal score of n^2 (n is the order of the grid), i.e., their cells can be completely filled. Like the 1800 PLSE benchmark instances, these 1800 LCS instances have an order $n \in \{50, 60, 70\}$ and ratio $r \in \{0.3, 0.4, 0.5, 0.6, 0.7, 0.8\}$, grouped to 18 subsets of 100 instances per (n, r) combination.

We ran the MPMA algorithm with a time limit of 3h with the parameters of Table 1 to solve the 1800 LCS instances. For the most difficult instances of the 19 traditional instances a time limit of 10 hours is required. The results on the set of 19 traditional instances (Table B.1) indicate that MPMA can solve all these instances with a perfect success rate. Only the best LSC algorithm MMCOL [14] reaches such a performance. However, MPMA requires a much higher computation time compared to the algorithm of [14].

Table B.2 displays the results of the MPMA algorithm on the set of 1800 LCS instances compared to the state-of-the-art algorithms [12,14] presented in Section 4.3. The results indicate that MPMA is able to solve all of these 1800 instances in the allotted time, matching the best LSC algorithm of [14].

Table B.1
Results of the MPMA algorithm on the set of 19 traditional LSC instances [9].

Instance			MPMA	
Name	n	r	SR	t(s)
qwhdec.order5.holes10.1	5	0.6	10/10	1.2
qwhdec.order18.holes120.1	18	0.63	10/10	1.9
qg.order30	30	0.0	10/10	22
qwhdec.order30.holes316.1	30	0.65	10/10	12
qwhdec.order30.holes320.1	30	0.64	10/10	4
qg.order40	40	0.0	10/10	55
qg.order60	60	0.0	10/10	526
qg.order100	100	0.0	10/10	3864
qwhdec.order35.holes405.1	35	0.67	10/10	56
qwhdec.order40.holes528.1	40	0.67	10/10	158
qwhdec.order60.holes1440.1	60	0.60	10/10	298
qwhdec.order60.holes1620.1	60	0.55	10/10	189
qwhdec.order70.holes2940.1	70	0.4	10/10	546
qwhdec.order70.holes2450.1	70	0.5	10/10	356
qwhdec.order33.holes381.bal.1	33	0.65	10/10	208
qwhdec.order50.holes825.bal.1	50	0.67	10/10	564
qwhdec.order50.holes750.bal.1	50	0.7	10/10	10546
qwhdec.order60.holes1080.bal.1	60	0.7	10/10	32484
qwhdec.order60.holes1152.bal.1	60	0.68	10/10	9556

Table B.2

Results of the MPMA algorithm on the 1800 new LSC instances [12] along with the results reported in the literature [12,14].

Instance		CPX-IP	CPX-CP	LSSOL	Tr-ILS*	MMCOL	MPMA
n	r	#Solved	#Solved	#Solved	#Solved	#Solved	#Solved
50	30	9	94	10	100	100	100
	40	3	71	8	100	100	100
	50	0	12	6	100	100	100
	60	0	0	0	36	100	100
	70	0	0	0	0	100	100
	80	100	100	100	100	100	100
60	0.3	0	71	1	100	100	100
	0.4	0	22	0	100	100	100
	0.5	0	1	0	95	100	100
	0.6	0	0	0	23	100	100
	0.7	0	0	0	0	100	100
	0.8	100	100	99	99	100	100
70	0.3	0	34	0	99	100	100
	0.4	0	8	0	98	100	100
	0.5	0	0	0	84	100	100
	0.6	0	0	0	10	100	100
	0.7	0	0	0	0	100	100
	0.8	100	100	46	98	100	100